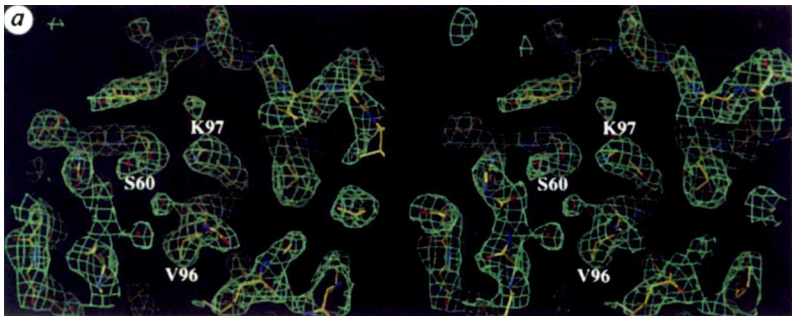

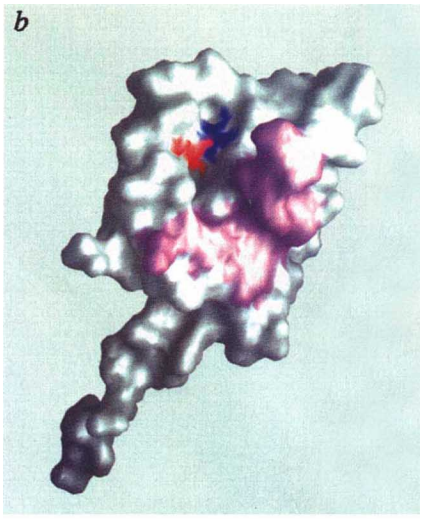

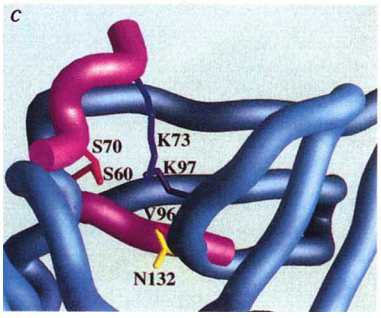

FIG. 3 *a*, Electron density representation of the active site residues Ser 60 and Lys 97, with a contour level of 1.2 σ. A stick model of the structure has been put into the density to show the relevant atoms and bonds. Water molecules are shown as red stars. *b*, A surface representation of the UmuD′ protein. The cleft leading to the active-site residues is clear in this representation. The surface contributed by the Ser 60 residue is coloured red and that by the Lys 97 residue is coloured blue. The residues that contribute to the molecular dimer interface have their surface contributions coloured violet (Tyr 52, Val 54, Ile 87, Gly 92, Glu 93, Phe 94, Phe 128). *c*, Worm representation of the UmuD′ backbone (yellow) with the sidechains of Ser 60 and Lys 97 in red and blue, respectively. The backbone carbonyl oxygen of residue Val 96 is in red. Superimposed are two segments of the TEM1 β-lactamase structure (in magenta). The first fragment includes residues 69–74 with the Ser 70 and the Lys 73 side chains in red and blue, respectively. The second fragment includes residues 129–133 with the Asn 132 side chain in yellow. An r.m.s. deviation of 0.12 Å is found when superimposing the Ser 60/Ser 70 Oγ, the Lys 97/Lys 73 Nε, and the Val 96 O with Asn 132 Oδ atoms. In the reaction proposed in ref. 17, Ser 70 Oγ attacks the carbonyl carbon of the β-lactam ring after activation by proton transfer to Lys 73 Nε, 2.7 Å away. The Lys 73 Nε is positioned by hydrogen bonds to the Asn 132 Oδ and the Ser 130 Oγ, holding the amino group in the proper conformation for catalysis. The TEM1 β-lactamase structure coordinates were kindly provided by N. Strynadka. Figures were generated in O[25] (*a*) and GRASP[30] (*b*, *c*).

(manuscript in preparation) and as such provides another example of how physiologically important quaternary interactions are maintained in the crystal lattice[18,19]. We propose that the UmuD′ filament probably forms a scaffold on the RecA–DNA filament that positions UmuC appropriately for interactions with the DNA polymerase III holoenzyme. The mutagenic character of UmuD necessitates that the protein be tightly regulated, with one level of regulation being the protein's activation by self-cleavage. Formation of the molecular dimer looks to be yet another regulatory mechanism for UmuD, blocking entry of the N terminus to the catalytic cleft, and preventing autodigestion. We are just beginning to understand that the small size of UmuD belies the multitude of interactions this protein has in its role in cell survival. □

Received 23 October 1995; accepted 4 March 1996.

1. Friedberg, E. C., Walker, G. C. & Siede, W. *DNA Repair and Mutagenesis* (ASM, Washington DC, 1995).
2. Rajagopalan, M. *et al. Proc. natn. Acad. Sci. U.S.A.* **89,** 10777–10781 (1992).
3. Woodgate, R. & Sedgwick, S. G. *Molec. Microbiol.* **6,** 2213–2218 (1992).
4. Little, J. W. *Proc. natn. Acad. Sci. U.S.A.* **81,** 1375–1379 (1984).
5. Gimble, F. S. & Sauer, R. T. *J. molec. Biol.* **192,** 39–47 (1986).
6. Shinagawa, H., Iwasaki, H., Kato, T. & Nakata, A. *Proc. natn. Acad. Sci. U.S.A.* **85,** 1806–1810 (1988).
7. Burckhardt, S. E., Woodgate, R., Scheuermann, R. H. & Echols, H. *Proc. natn. Acad. Sci. U.S.A.* **85,** 1811–1815 (1988).
8. Nohmi, T., Battista, J. R., Dodson, L. A. & Walker, G. C. *Proc. natn. Acad. Sci. U.S.A.* **85,** 1816–1820 (1988).
9. Peat, T. S., Frank, E. G., Woodgate, R. & Hendrickson, W. A. *Proteins* (in the press).
10. Hendrickson, W. A. *Science* **254,** 51–58 (1991).
11. Hendrickson, W. A., Horton, J. R. & LeMaster, D. M. *EMBO J.* **9,** 1665–1672 (1990).
12. Lin, L.-L. & Little, J. W. *J. molec. Biol.* **210,** 439–452 (1989).
13. Battista, J. R., Ohta, T., Nohmi, T., Sun, W. & Walker, G. C. *Proc. natn. Acad. Sci. U.S.A.* **87,** 7190–7194 (1990).
14. Roland, K. L., Smith, M. H., Rupley, J. A. & Little, J. W. *J. molec. Biol.* **228,** 395–408 (1992).
15. Gimble, F. S. & Sauer, R. T. *J. molec. Biol.* **206,** 29–39 (1989).
16. Little, J. W. *J. Bact.* **175,** 4939–4950 (1993).
17. Strynadka, N. C. J. *et al. Nature* **359,** 700–705 (1992).
18. Story, R.M., Weber, I. T. & Steitz, T. A. *Nature* **355,** 318–325 (1992).
19. Shapiro, L. *et al. Nature* **374,** 327–337 (1995).
20. Studier, F. W., Rosenberg, A. H., Dunn, J. J. & Dubendorf, J. W. *Meth. Enzym.* **185,** 60–89 (1990).
21. Otwinowski, Z. in *DENZO* (eds Sawyer, L., Isaacs, N. & Bailey, S.) 56–62 (SERC Daresbury Laboratory, Warrington, UK, 1993).
22. Collaborative Computational Project no.4 *Acta crystallogr.* D**50,** 760–763 (1994).
23. Debaerdemaeker, T. *et al. MULTAN 88 Acta crystallogr.* **A44,** 353–357 (1988).
24. Brunger, A. T. *XPLOR, Version 3.1, A System for X-ray Crystallography and NMR* (Yale Univ. Press, New Haven, 1992).
25. Jones, T. A., Zou, J.-Y., Cowan, S. W. & Kjeldgaard, M. *Acta crystallogr.* A**47,** 110–119 (1991).
26. Kleywegt, G. J. & Jones, T. A. *From First Map to Final Model* (eds Bailey, S. H. R. & Walker, R.) 59–66 (SERC Daresbury Laboratory, Warrington, UK, 1994).
27. Laskowski, R. A., MacArthur, M. W., Moss, D. S. & Thornton, J. M. *J. appl. Crystallogr.* **26,** 283–291 (1993).
28. Evans, S. V. *J. molec. Graphics* **11,** 134–138 (1990).
29. Kraulis, P. J. *J. appl. Crystallogr.* **24,** 946–950 (1991).
30. Nicholls, A., Sharp, K. A. & Honig, B. *Proteins* **11,** 281–296 (1991).

ACKNOWLEDGEMENTS. We thank J. Newman, L. Shapiro and C. Ogata for help with data collection, analysis and subsequent structure solution. This work was supported in part by a grant from the NIH. Beamline X4A at the National Synchrotron Light Source, a DOE facility, is supported by the Howard Hughes Medical Institute. Coordinates have been deposited in the Protein Data Bank, Brookhaven (accession number 1umu).

CORRESPONDENCE and requests for materials should be addressed to W.A.H. (e-mail: hendw@cuhhca.hhm.columbia.edu

Context-dependent secondary structure formation of a designed protein sequence

Daniel L. Minor Jr* & Peter S. Kim†

Howard Hughes Medical Institute, Whitehead Institute for Biomedical Research, Departments of * Chemistry and † Biology, Massachusetts Institute of Technology, Nine Cambridge Center, Cambridge, Massachusetts 02142, USA

PROTEIN secondary structures have been viewed as fundamental building blocks for protein folding, structure and design. Previous studies indicate that the propensities of individual amino acids to form particular secondary structures are the result of a combination of local conformational preferences[1,2] and non-local factors[3–7]. To examine the extent to which non-local factors influence the formation of secondary structural elements, we have designed an 11-amino-acid sequence (dubbed the 'chameleon' sequence) that folds as an α-helix when in one position but as a

β-sheet when in another position of the primary sequence of the IgG-binding domain of protein G (GB1). Both proteins, chameleon-α and chameleon-β, are folded into structures similar to native GB1, as judged by several biophysical criteria. Our results demonstrate that non-local interactions can determine the secondary structure of peptide sequences of substantial length. They also support views of protein folding that favour tertiary interactions as dominant determinants of structure (for example, see refs 8,9).

The 'chameleon' sequence (Chm) was designed to replace α-helix residues 23–33 and β-sheet residues 42–52 (Fig. 1*a*) of GB1. Our aim was to preserve the hydrophobic nature of the residues that constitute the interface between each of these secondary structure elements and the core of GB1 (Fig. 1*b*). As the characteristic hydrophobic/hydrophilic patterning of buried residues in α-helices and β-sheets is very different, with periodicities of 3.6 and 2 residues respectively, creation of a sequence consistent with both patterns posed a number of design problems.

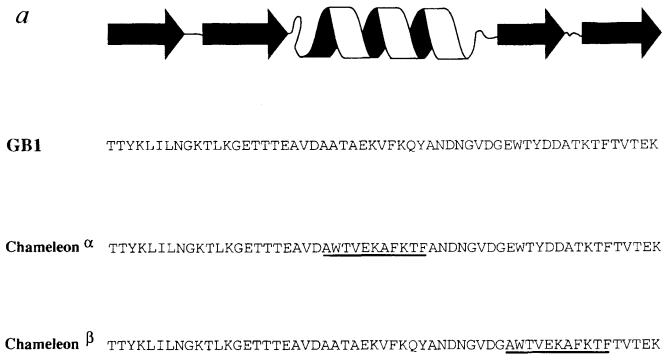

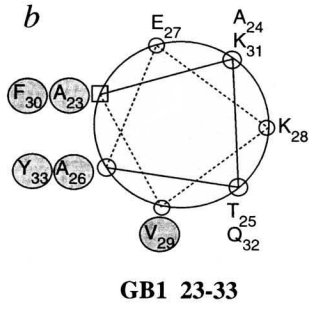

GB1 23-33

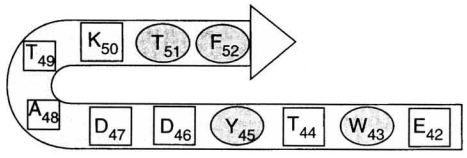

GB1 42-52

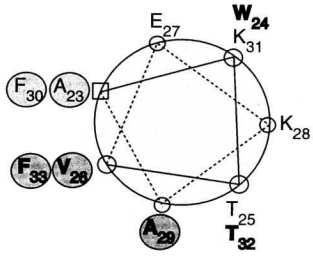

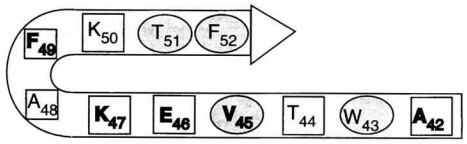

Chameleonβ 42-52

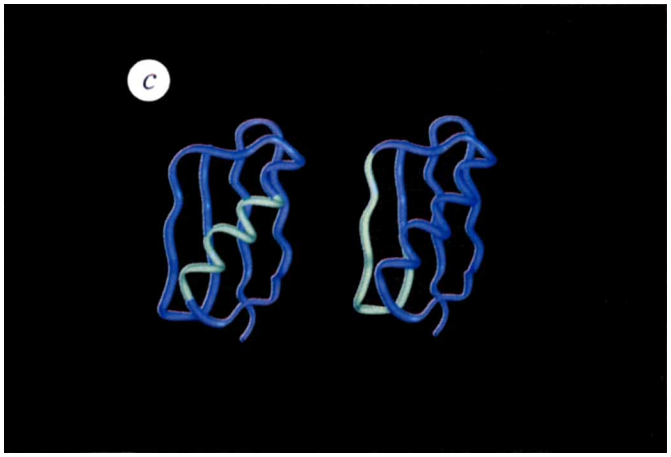

FIG. 1 *a*, GB1 secondary structure. The primary amino-acid sequences of GB1, Chm-α and Chm-β are positioned below the corresponding secondary structures. *b*, Positions 23–33 and 42–52 of GB1 and Chm sequences. Changes from wild-type sequence are indicated in bold. Residues involved in the interface between each secondary structure and the remainder of the protein are shaded. *c*, Ribbon diagram showing the Chm sequence in Chm-α (left) and Chm-β (right); the Chm sequence is shown in yellow. The diagram was drawn using the coordinates of wild-type GB1 (ref. 21).

METHODS. GB1 mutants were derived from a synthetic GB1 gene by site-directed mutagenesis, verified by dideoxyribonucleotide sequencing, expressed in *E. coli* and purified by IgG-affinity chromatography and reverse-phase HPLC (ref. 22). In the GB1 homologue GB2 (ref. 23), position 57 is incorporated as part of the fourth β-strand. GB1*, with residue K57 added to the 56-residue construct GB1-Thr1 (ref. 22), had a $T_m \sim 2$ °C higher than GB1-Thr1 and was used as the parent construct for all Chm proteins. Molecular identities were verified by matrix-assisted laser desorption/ionization (MALDI) mass spectrometry (Finnigan MAT Lasermat or PerSeptive Biosystems Voyager) and found to be within 2 daltons of the expected mass for the 57-residue protein. The Chameleon sequence positions 23, 26, 30 and 33 were judged to be important for the helix–protein interface, whereas positions 43, 45, 51 and 52 were judged to be important for the β-sheet–protein interface (see text). For all class I sites, the buried residue was used, with the exception of the 29/48 pair. The buried residue of the 29/48 pair was not used as T49F was a necessary change in the turn between strands III and IV of Chm-β to preserve the buried Phe from the 30/49 class I pair, and we did not wish to cause two sequential amino-acid changes in this turn. We tested a number of substitutions for pair 26/45 in GB1*. The T_m (ΔH_m) values from thermal unfolding were: A26Y, < 0 °C (not determined); A26I, 59.6 °C (42.5 kcal mol^{-1}); A26V, 66.5 °C (50.9 kcal mol^{-1}); Y45A, 53.4 °C (40.4 kcal mol^{-1}); Y45V, 61.1 °C (47.5 kcal mol^{-1}); Y45I, 61.8 °C (44.5 kcal mol^{-1}); thus Val was chosen for the 26–45 pair. Constructs containing a 10-residue Chm sequence at positions 23–32 and 42–51 of GB1* were seen to fold, so the 33/52 pair was examined. Substitution of Y33F lowered the T_m of the α-helix Chm by 0.6 °C, whereas F52Y lowered the T_m of the β-sheet Chm by 8.7 °C. Phe was chosen for the 33/52 pair in Chm-α and Chm-β.

In comparing the structural environments of positions 23–33 and 42–52, we encountered three main types of environments based on accessible surface area: class I, sites where a residue was buried in one secondary structure but exposed in the other (pairs 23/42; 24/43; 29/48; 30/49 and 32/51; the buried residue is underlined); class II, sites where a residue occupied a buried position in both structures but was very different in size or polarity in each structure (pairs 26/45 and 33/52); and class III, sites that had no conflicts in terms of size, polarity or burial (pairs 25/44; 27/46; 28/47 and 31/50). For class I sites, the buried residue from each pair was used for the Chm sequence, with the exception of pair 29/48 (Fig. 1 legend). For class II sites, a series of hydrophobic

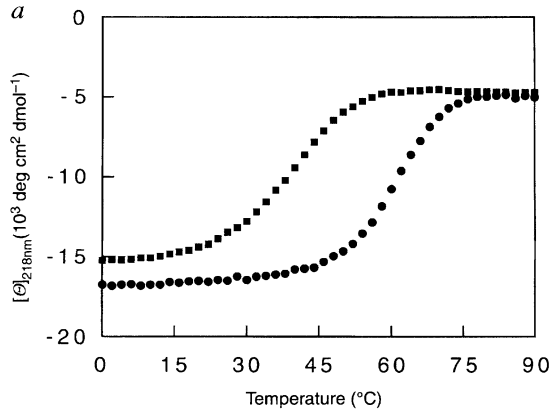

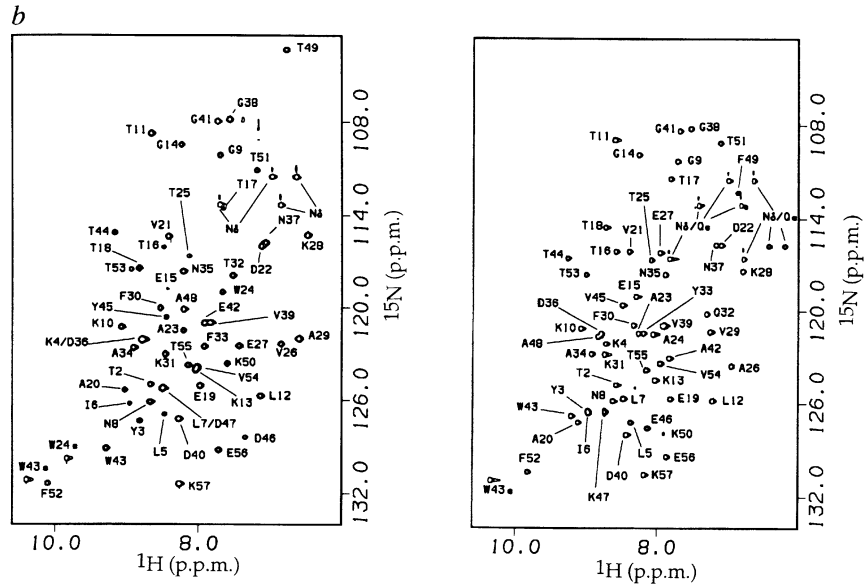

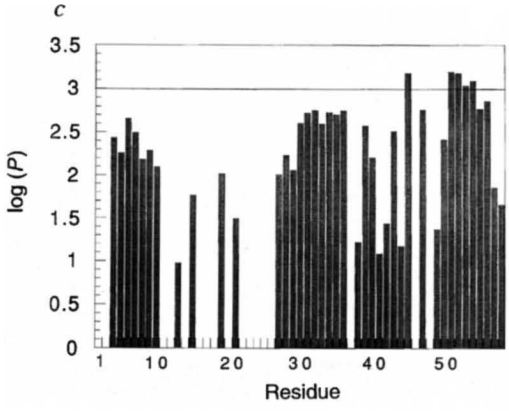

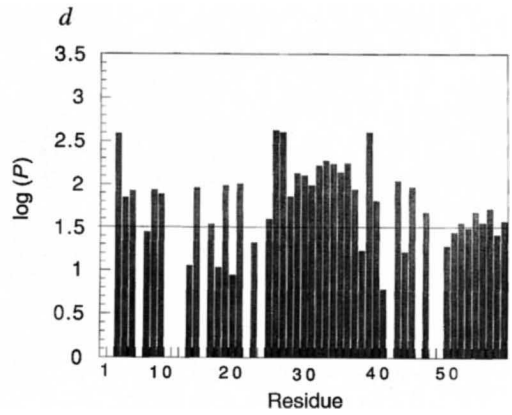

FIG. 2 *a*, Thermal denaturation of Chm-α (circles) and Chm-β (squares) in 150 mM NaCl, 50 mM sodium acetate, pH 5.4. T_m (ΔH_m) values are: Chm-α, 61.4 °C (41.5 kcal mol^{-1}); Chm-β, 39.2 °C (27.7 kcal mol^{-1}). T_m (ΔH_m) values for wild-type GB1 are 87.5 °C (61.7 kcal mol^{-1})[24]. From differential scanning calorimetry (DSC), $\Delta H_{cal} = 44.1$ kcal mol^{-1} ($\Delta H_{cal}/\Delta H_{van't\ Hoff} = 1.06$) for Chm-α, consistent with two-state unfolding. DSC of Chm-β gave an unsatisfactory folded baseline at 0–10 °C. *b*, ^{1}H–^{15}N correlation spectra of Chm-α (left) and Chm-β (right) proteins at 5 °C, pH 5.4 (10% D_2O). Labels indicate resonance assignments. The side-chain resonances are labelled as Nδ/Qε. At lower contours, the heteronuclear single quantum coherence (HSQC) spectra of Chm-β contain a set of small amide peaks at chemical shifts characteristic of unfolded polypeptides[25] which increase in size as the temperature is raised, suggesting that they arise from the unfolded state, in slow exchange with the folded state on the NMR timescale. Measurement of the amide-proton peak volumes indicates that ~ 1–3% of the molecules are unfolded at 5 °C, as expected from the ΔG of folding for Chm-β. *c*, Amide-proton protection patterns for Chm-α (*c*) and Chm-β (*d*). *P* is the protection factor from exchange, defined as k_{rc}/k_{obs}, where k_{rc} is the hydrogen-exchange rate expected in a random coil and corrected for primary structure effects[26], and k_{obs} is the measured hydrogen-exchange rate. Horizontal lines indicate the log (*P*) value expected from the global stability of each protein at 5 °C (see also ref. 27).

METHODS. CD thermal unfolding and DSC measurements were made as described[22]. NMR experiments and resonance assignments were done with ^{15}N-labelled protein[22]. For hydrogen exchange experiments, fully protonated Chm-α and Chm-β were adjusted to pH 5.4 and lyophilized from water. Exchange was initiated by dissolution into exchange buffer, 50 mM acetic-d_3-acid-d (Aldrich 99.5 atom % D) in D_2O (Aldrich 100.0 atom % D), pH 5.4 at 5 °C (measured in D_2O using a glass electrode without correction for isotope effects). Proton occupancy was measured from ^{1}H–^{15}N HSQC spectra with 2, 4, 16 or 32 transients per increment, with 100 T1 increments. Amide-proton decay was measured from peak volumes in ^{1}H–^{15}N HSQC spectra using FELIX230 (Biosym). Amide-proton-exchange rates were calculated using $I(t) = e^{(-kt)} + I(\infty)$, where $I(t)$ is intensity at time t and k is the measured exchange rate. $I(\infty)$ values were all 0 ± 0.1. The protection factor P was calculated to account for primary sequence effects[26]. The global stability of each protein at 5 °C was calculated from CD thermal unfolding measurements and the Gibbs–Helmholtz equation[22].

residues were substituted at the positions of the residue pairs in the wild-type GB1 background in order to find a common residue for both environments that did not disrupt protein stability too drastically (Fig. 1 legend). After determining the residues that would enable a single sequence to fulfil the tertiary requirements of both positions 23–33 and 42–52 in GB1 using this procedure, the sequence AWTVEKAFKTF was introduced at positions 23–33 or 42–52 of GB1 by site-directed mutagenesis, thereby creating the proteins Chm-α and -β, respectively (Fig. 1*c*).

Chameleon-α and -β each display cooperative reversible thermal unfolding as measured by circular dichroism (CD) spectroscopy (Fig. 2*a*) and differential scanning calorimetry experiments (Fig. 2 legend). This type of thermal unfolding behaviour is a hallmark of compact single-domain globular proteins with uniquely packed hydrophobic cores[10].

The NMR spectra of Chm-α and Chm-β have substantial chemical-shift dispersion (Fig. 2*b*). In addition, NMR-detected hydrogen-exchange experiments indicate that both proteins contain a set of backbone amides that have exchange rates equal to or slower than those expected for exchange occurring only from global unfolding (Fig. 2*c*, *d*). Together with the thermal unfolding data, these results strongly suggest that both Chm proteins have unique folded structures with well packed hydrophobic cores (see discussion in ref. 11).

Nuclear Overhauser (NOE) spectra indicate that, as designed, the Chm sequence is folded into an α-helix in Chm-α (Fig. 3*a*) and a β-strand/turn/β-strand in Chm-β (Fig. 3*b*). In both proteins, amide protons from residues in the Chm sequence are significantly protected from hydrogen exchange, indicating that the hydrogen bonds in each secondary structure formed by the Chm sequence are stable.

NOE patterns throughout each protein are consistent with those in wild-type GB1 (Fig. 4). Furthermore, Chm-α and Chm-β are capable of competing for Fc binding with wild-type GB1, although with somewhat reduced affinities (Fig. 4 legend). The amino-acid changes in Chm-α and Chm-β occur in regions of the protein that have been identified as part of the Fc binding interface[12], so it is likely that much of the affinity differences are the result of mutation of interface residues. Considered together with the NMR data, the fact that Fc binding can occur strongly suggests that both Chm proteins are folded into structures similar to wild-type GB1.

As some short isolated peptides can form significant amounts of secondary structure[1,13], an 11-residue peptide corresponding to the Chm sequence (Ac-AWTVEKAFKTF-NH_2, where Ac is acetyl) was synthesized to investigate whether this sequence could have any intrinsic conformational preferences. Both CD and NMR indicate that the Chm peptide is unfolded in isolation (Fig. 4 legend), suggesting that the Chm primary sequence itself has no strong preference for either the α-helix or β-sheet conformation. Thus, the secondary structure formed by the Chm sequence in both Chm-α and Chm-β proteins is specified by tertiary interactions.

The secondary structure of peptide sequences in some natural proteins, such as haemagglutinin and the serpins, undergo major conformational alterations following tertiary rearrangements induced by pH changes or proteolytic cleavage[14–16]. Tertiary interactions play a dominant role in determining the propensity of individual amino acids to form β-sheets[3,5,7]; they also affect the secondary structure conformation of identical short peptide sequences (up to 6 amino acids long) in proteins in the structural database[17–20]. Our Chm sequence design demonstrates directly

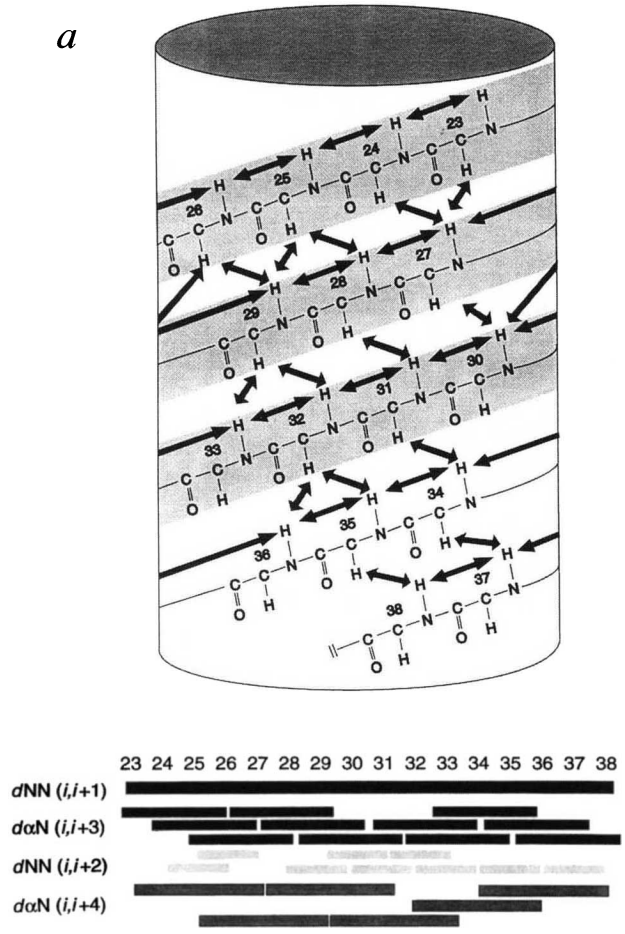

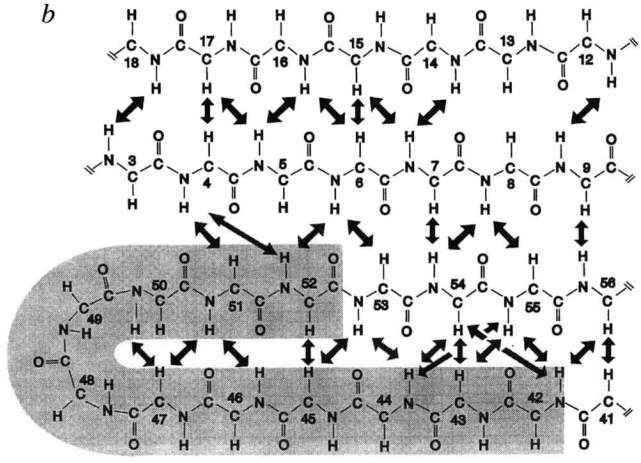

FIG. 3 Nuclear Overhauser effects (NOEs) attributable to *a*, the α-helical, and *b*, the β-sheet conformations of the Chm sequence (highlighted in grey) in Chm-α and Chm-β. NOEs in Chm-α indicative of helical structure are indicated as bars in *a*. Cross-strand NOEs in Chm-β are indicated by arrows in *b* and include: H^N_{44}–H^N_{53}, H^N_{44}–H^N_{55}, H^α_4–H^N_{52}, H^N_8–H^N_{54}, H^N_{46}–H^N_{51}, H^N_9–H^N_{12}, H^α_{45}–H^α_{52}, H^α_{43}–H^α_{54}, H^α_6–H^α_{15}, H^α_4–H^α_{17}, H^α_{45}–H^N_{53}, H^N_5–H^α_{17}, H^N_6–H^α_{53}, H^α_{43}–H^N_{55}, H^α_6–H^N_{16}, H^N_4–H^α_{51}, H^N_7–H^α_{15}, H^N_6–H^N_{52}, H^N_7–H^N_{14}, H^N_{42}–H^N_{55}, H^N_{42}–H^α_{56}, H^N_3–H^N_{18}, H^α_{41}–H^α_{56}, H^α_{47}–H^N_{51}, H^N_5–H^N_{16}, H^α_4–H^α_{51}, H^α_4–H^γ_{17}, H^γ_7–H^N_{54}, H^N_8–H^α_{55}, H^N_{44}–H^α_{54}, H^α_9–H^N_{56}, H^α_{47}–H^N_{50}, $H^{\gamma 1}_{54}$–H^N_{43}, $H^{\gamma 1}_{54}$–H^δ_{43}, $H^{\gamma 1}_{54}$–$H^{\zeta 2}_{43}$, $H^{\gamma 1}_{54}$–H^N_{42}, $H^{\gamma 1}_{54}$–H^N_{41}, $H^{\gamma 1}_{54}$–H^N_{44}, $H^{\gamma 2}_{54}$–H^N_{52}, $H^{\gamma 2}_{54}$–H^N_{44}, $H^{\gamma 2}_{54}$–H^δ_{43}, $H^{\gamma 2}_{54}$–$H^{\zeta 2}_{43}$. NMR measurements were made as described[22] and included NOESY spectra with 150-ms mixing times.

FIG. 4 Diagram of tertiary NOEs observed between the helix and sheet in both Chm-α and Chm-β. Tertiary NOEs represented by the arrows include: $H^{\beta}_{34} - H^{\beta}_{54}$, $H^{\beta}_{34} - H^{\gamma 1}_{54}$, $H^{\beta}_{34} - H^{\gamma 2}_{54}$, $H^{\gamma 1}_{26} - H^{\beta}_{3}$, $H^{\gamma 1}_{26} - H^{\beta}_{3}$, $H^{\gamma 2}_{26} - H^{\alpha}_{3}$, $H^{\rho 2}_{43} - H^{N}_{31}$, $H^{\rho 2}_{43} - H^{\alpha}_{31}$, $H^{\eta 2}_{43} - H^{N}_{30}$, $H^{\beta}_{34} - H^{\eta 2}_{43}$, $H^{\beta}_{34} - H^{\rho 2}_{43}$, for Chm-α; $H^{\rho 2}_{43} - H^{N}_{31}$, $H^{\eta 2}_{43} - H^{N}_{30}$, $H^{\beta}_{34} - H^{\gamma}_{54}$, $H^{\beta}_{34} - H^{\eta 2}_{43}$, $H^{\beta 1}_{3} - H^{\beta}_{26}$, $H^{\beta 2}_{3} - H^{\beta}_{26}$ for Chm-β. Competitive Fc binding experiments with GB1* indicate that both proteins bind Fc. Chm-α and Chm-β have relative dissociation constants (K_d/K_d^{GB1}) for Fc binding of 12.0 and 36.0, respectively; K_d for wild-type GB1 is 7.1 nM[28]. Binding was assayed at 4 °C as described[22]. Sedimentation equilibrium give values for relative molecular masses (M_rs) of 6,800 (calculated, 6,366) and 6,500 (calculated, 6,246) for Chm-α and Chm-β, respectively with random residuals, indicating that both are monomeric. The observed M_rs were independent of protein concentration (10–100 μM). A peptide, Ac-AWTVEKAFKTF-NH_2, corresponding to the Chm sequence with blocked ends, was examined. Its CD spectrum at 0 °C had features typical of unfolded polypeptides[29], was independent of concentration (10–200 μM) and the temperature dependence of the signal at 222 nm was linear from 0–70 °C (data not shown). NMR spectra showed chemical shift dispersion typical of unstructured peptides[25]. Chou–Fasman[30] values for the Chm sequence ($\langle P_\alpha \rangle = 1.15$ and $\langle P_\beta \rangle = 1.05$) indicate that this sequence has no strong statistical preference for α-helix or β-sheet formation.

METHODS. Sedimentation equilibrium measurements were made as described[9] at rotor speeds of 35,000 and 42,000 r.p.m. at 4 °C in 150 mM NaCl, 50 mM sodium acetate, pH 5.4. Dilutions were made into dialysate to obtain 10–100 μm protein samples. Apparent M_rs were calculated by fitting data sets from each sector to a single ideal species model. Partial specific volumes of 0.7323 and 0.7406 ml g^{-1} were used for Chm-α and Chm-β, respectively, and corrected for temperature[31]. The Chm peptide was synthesized by solid-phase Fmoc methods (Applied Biosystems peptide synthesizer 431A) and purified by Sephadex G-25 size-exclusion chromatography in 5% acetic acid and reverse-phase HPLC purification (on a Vydac C18 column using linear H_2O-acetonitrile gradients and 0.1% trifluoroacetic acid). Chm peptide identity was confirmed by MALDI mass spectrometry, measured as 1,367 (expected, 1,368) daltons. CD spectra of Chm peptide were run in 150 mM NaCl, 50 mM sodium acetate, pH 5.4; NMR spectra were obtained in 10% D_2O, pH 5.4.

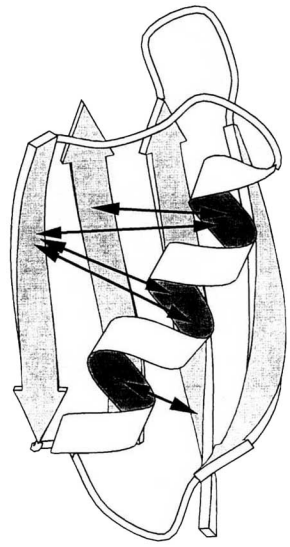

that the information specifying α-helix or β-sheet secondary structures can be entirely non-local. Taken together, these results underscore the importance of context-dependent effects in protein folding. □

Received 14 December 1995; accepted 23 February 1996.

1. Chakrabartty, A. & Baldwin, R. L. *Adv. Prot. Chem.* **46,** 141–176 (1995).
2. Bryson, J. W. *et al. Science* **270,** 935–941 (1995).
3. Garratt, R. C., Taylor, W. R. & Thornton, J. M. *FEBS Lett.* **188,** 59–62 (1985).
4. Heinz, D. W., Baase, W. A., Dahlquist, F. W. & Matthews, B. W. *Nature* **361,** 561–564 (1993).
5. Minor, D. L. Jr & Kim, P. S. *Nature* **371,** 264–267 (1994).
6. Xiong, H., Buckwalter, B. L., Shieh, H.-M. & Hecht, M. H. *Proc. natn. Acad. Sci. U.S.A.* **92,** 6349–6353 (1995).
7. Smith, C. K. & Regan, L. *Science* **270,** 980–982 (1995).
8. Dill, K. A. *et al. Prot. Sci.* **4,** 561–602 (1995).
9. Lumb, K. J., Carr, C. M. & Kim, P. S. *Biochemistry* **33,** 7361–7367 (1994).
10. Privalov, P. L. *A. Rev. Biophys. biophys. Chem.* **18,** 47–69 (1989).
11. Lumb, K. J. & Kim, P. S. *Biochemistry* **34,** 8642–8648 (1995).
12. Gronenborn, A. M. & Clore, G. M. *J. molec. Biol.* **223,** 331–335 (1993).
13. Dyson, H. J. & Wright, P. E. *A. Rev. Biophys. biophys. Chem.* **20,** 519–538 (1991).
14. Carr, C. M. & Kim, P. S. *Cell* **73,** 823–832 (1993).
15. Bullough, P. A., Hughson, F. M., Skehel, J. J. & Wiley, D. C. *Nature* **371,** 37–43 (1994).
16. Goldsmith, E. J. & Mottonen, J. *Structure* **2,** 241–244 (1994).
17. Kabsch, W. & Sander, C. *Proc. natn. Acad. Sci. U.S.A.* **81,** 1075–1078 (1984).
18. Wilson, I. A., Haft, D. H., Getzoff, E. D., Tainer, J. A. & Lerner, R. A. *Proc. natn. Acad. Sci. U.S.A.* **82,** 5255–5259 (1985).
19. Argos, P. *J. molec. Biol.* **197,** 331–348 (1987).
20. Cohen, B. I., Presnell, S. R. & Cohen, F. E. *Prot. Sci.* **2,** 2134–2145 (1993).
21. Gronenborn, A. M. *et al. Science* **253,** 657–661 (1991).
22. Minor, D. L. Jr & Kim, P. S. *Nature* **367,** 660–663 (1994).
23. Achari, A. *et al. Biochemistry* **31,** 10449–10457 (1991).
24. Alexander, P., Fahnestock, S., Lee, T., Orban, J. & Bryan, P. *Biochemistry* **31,** 3597–3603 (1992).
25. Wüthrich, K. *NMR of Proteins and Nucleic Acids* (Wiley, New York, 1986).
26. Bai, Y., Milne, J. S., Mayne, L & Englander, S. W. *Proteins* **17,** 75–86 (1993).
27. Orban, J., Alexander, P., Bryan, P. & Khare, D. *Biochemistry* **34,** 15291–15300 (1995).
28. Fahnestock, S. R., Alexander, P., Filpula, D. & Nagle, J. in *Bacterial Immunoglobin-binding Proteins* (ed. Boyle, M. D. P.) (Academic, San Diego, 1990).
29. Woody, R. W. in *The Peptides* (Academic, New York, 1985).
30. Chou, P. Y. & Fasman, G. D. *Biochemistry* **13,** 211–222 (1973).
31. Schuster, T. M. & Laue, T. M. *Modern Analytical Ultracentrifugation* (Birkhäuser, Boston, 1994).

ACKNOWLEDGEMENTS. We thank L. M. Mayr, C. J. McKnight, Z. Y. Peng, P. A. Petillo, B. A. Schulman and T. N. M. Schumacher for advice and discussion, and A. G. Cochran, B. A. Schulman, T. N. M. Schumacher, R. Rutkowski and R. T. Sauer for comments on the manuscript.

CORRESPONDENCE AND MATERIALS. Requests to be addressed to P.S.K.

RETRACTION

Long-term correction of rat model of Parkinson's disease by gene therapy

Shoushu Jiao, Vladimir Gurevich & Jon A. Wolff

Nature **362,** 450–453 (1993)

J.A.W. writes — In my laboratory we have been attempting to extend the findings reported in this paper. During these efforts, it has come to my attention that the pertinent laboratory notebooks were replaced with edited text and data. An independent analysis of the remaining original data revealed that the published Fig. 2*b* and *c* contains errors that exaggerate both the reductions in the number of rotations after transplantation and the increments in the numbers of rotations following graft removal. Review of the protocol reported in the legend to Fig. 2 indicates that control transfections were done using TransfectACE (Promega) instead of Lipofectin (BRL), which may have affected the outcome of the experiments. Subsequent experiments have failed to replicate the original observations. Regrettably, therefore, I am unable to verify that the conclusions of this paper are correct. □